Optimal skirt spacing for subsea mudmats under loading in six degrees of freedom

X. Feng[1], S. Gourvenec[1] and M. F. Randolph[1]

Published in *Applied Ocean Research,* Vol. 48, October 2014, 10–20.

http://dx.doi.org/10.1016/j.apor.2014.07.006

[1]Xiaowei FENG (corresponding author)
Centre for Offshore Foundation Systems – M053
University of Western Australia
35 Stirling Highway, Crawley
Perth, WA 6009
Australia
Tel: +61 8 6488 2473
Fax: +61 8 6488 1044
Email: xiaowei.feng@uwa.edu.au

[1]Susan GOURVENEC
Centre for Offshore Foundation Systems
University of Western Australia
Tel: +61 8 6488 3094
Email: susan.gourvenec@uwa.edu.au

[1]Mark F. RANDOLPH
Centre for Offshore Foundation Systems
University of Western Australia
Tel: +61 8 6488 3075
Email: mark.randolph@uwa.edu.au

No. of words: 4074 (without abstract and references)
No. of tables: 2
No. of figures: 16

Optimal skirt spacing for subsea mudmats under loading in six degrees of freedom

X. Feng[1], S. Gourvenec[1] and M.F. Randolph[1]

ABSTRACT

Two- and three- dimensional finite element analyses are performed to identify the optimal internal skirt spacing for the maximum undrained capacity of subsea skirted mudmats. Fully three-dimensional loading (vertical, biaxial horizontal, biaxial moment and torsion) is considered for subsea mudmats with skirt embedment ranging from 5 to 20% of the foundation breadth in soil with a range of linearly increasing strength with depth. The results have identified the governing case for determining the optimal skirt spacing for mudmats subjected to fully three-dimensional loading. It is also shown that optimal skirt spacing for rectangular or square mudmats can be determined in plane strain conditions using the equivalent foundation embedment ratio. The number of internal skirts required to ensure soil plug rigidity under fully three-dimensional loading is presented as a function of skirt embedment ratio, soil heterogeneity index and vertical load mobilisation. Results also indicate that effects of skirt roughness become negligible as foundation embedment increases in terms of determining the optimal skirt spacing.

KEYWORDS

Seabed foundations; bearing capacity; failure; numerical modelling; offshore engineering; torsion

[1] Centre for Offshore Foundation Systems, The University of Western Australia

1. INTRODUCTION

With the exploration and exploitation of offshore oil and gas moving into deep and ultra-deep water, skirted mudmat foundations have been increasingly deployed on the seabed to support subsea structures such as pipeline end terminations (PLETs) and in-line structures. Skirted mudmat foundations typically consist of a rectangular plate (i.e. the mat), fitted with perimeter and internal skirts. Penetration of the skirts into stronger soil below the mudline increases capacities of skirted mudmat foundations compared with surface foundations.

Capacity of skirted foundations can be compromised if insufficient internal skirts are provided, as soil failure mechanisms can occur within the soil plug under certain loading and soil conditions. So-called 'internal mechanisms' are most prone to occur in foundations with low embedment ratio and soils with high strength heterogeneity. In these cases, the average strength within the soil plug is lower than the strength of soil beneath foundation level (i.e. at skirt-tip level), providing a path of lower resistance for the failure mechanism within the soil plug.

The response of shallowly embedded foundations to combined vertical load (V), moment (M) and horizontal load (H) has been investigated previously by means of finite element (FE) and upper bound plasticity analysis, see e.g. Refs. [1, 2, 6, 8, 9, 18]. These studies can be applied to skirted foundations on the assumption that sufficient internal skirts are provided so that the soil plug enclosed by the perimeter skirts displaces as an intact body with the foundation during loading. The potential reduction in foundation capacity resulting from internal mechanisms has been demonstrated for particular soil and loading conditions, see e.g. Refs. [3, 12].

The role of internal skirts has received greater attention recently in response to the increased use of skirted mudmat foundations in deepwater seabeds, which typically comprise soft normally consolidated or lightly over consolidated sediments. The high strength gradients at shallow depth increase the tendency for internal mechanisms between the skirts.

A simple method to determine the minimum skirt spacing for skirted foundations to resist significant lateral loads is proposed in a marine geotechnical handbook [17] and recommends a spacing no greater than 1.0d in cohesive soil (where d the skirt depth as depicted in Figure 1). The method does not extend to general combined loading conditions and the recommended spacing is considerably closer than commonly adopted in practice. A

systematic study of optimal skirt spacing has been proposed for skirted foundations under combined in-plane V-M-H loading, but the study was restricted to conditions of plane strain and to only the limits of soil strength heterogeneity [11]. Subsea mudmats are generally three-dimensional in geometry and subjected to loading in six degrees-of-freedom (see Figure 1), namely vertical load (V), biaxial horizontal load (H_x, H_y), biaxial moment (M_y, M_x) and torsion (T), referred to here as V-H^2-M^2-T loading. The generality of previous findings based on the in-plane V-M-H loading should therefore to be verified. V-H^2-M^2-T load capacity of square skirted mudmats was investigated for limiting cases of soil strength heterogeneity [5], but to date there has been no systematic study to define optimal skirt spacing across a full range of foundation aspect ratios and embedment ratios for practical intervals of soil strength heterogeneity.

The work presented in this paper identifies the optimal skirt spacing of subsea mudmats for maximum capacity (i) under fully three-dimensional loading conditions, (ii) over the range of plan geometry from strip to square, (iii) embedment ratios from 5 – 20% of the foundation breadth, (iv) and at practical intervals of soil strength heterogeneity over the full range from uniform with depth to essentially normally consolidated. The load-carrying capacities of skirted mudmats under fully combined loading conditions are presented in the form of failure envelopes and the optimal skirt spacing is defined by comparing the failure envelopes obtained from parallel analyses of the skirted and solid embedded foundations. Design charts are proposed for determining the optimal skirt spacing as a function of foundation aspect ratio, foundation embedment ratio, soil heterogeneity index and the vertical load mobilisation.

2. FINITE ELEMENT MODEL

All the finite element analyses presented from this study were carried out using the commercially available software Abaqus [4].

2.1 Geometry and meshes

The three-dimensional finite element mesh used for the analysis of a typical rectangular mudmat with breadth-to-length aspect ratio of B/L = 0.5 is shown in Figure 2 (half view). The breadth (side length for a square mudmat) was taken as B = 5 m for all of the analysis, but the results are presented as normalised quantities so that they are independent of the selected foundation size. The meshes extended 3B from the edges of the foundation and 3B beneath the foundation base (or skirt tip) level, with horizontally constrained nodes at the sides, and fully constrained nodes at the base. The boundaries were shown to be sufficiently remote so

that the failure mechanism was not affected. A region of very thin elements was provided at foundation level (approximately 0.3%B) to ensure accurate representation of shearing, especially with high soil strength heterogeneity. The meshes for the square mudmat foundations maintained the same geometry and discretisation on the central plane (i.e. the front face in Figure 2) as for the rectangular mudmats. Fewer elements were used for square foundations in the longitudinal direction in order to maintain a consistent element size across the models. Linear 8-node brick hybrid elements were used for the rectangular and square foundation models. The hybrid element formulation uses a mixture of displacement and stress variables (as opposed to solely displacement) to approximate the equilibrium equations and compatibility conditions. Hybrid elements are recommended for modelling the response of in compressible and near-incompressible materials (such as is appropriate for undrained soil conditions).

A plane strain mesh was constructed using 4-node quadrilateral hybrid elements. The same geometry and discretisation as for the front face of the three-dimensional mesh as shown in Figure 2 was used, and equivalent boundary conditions, soil conditions and analysis procedures were modelled as in the three dimensional analyses.

The foundations were modelled as a solid plug or skirted foundations with a number, n, of internal skirts ($0 \leq n \leq 8$). The foundation, whether a solid plug or skirted, was modelled as a rigid body with a load reference point (LRP) defined at the centroid of the foundation at mudline level. In the analyses, all foundation loads and displacements were applied or recovered at this point. Internal skirts, where provided, were implicitly modelled by constraining the mesh nodes at the relevant location(s) using the kinematic coupling constraint method, as shown schematically in Figure 3. The constrained nodes were coupled to the LRP such that the motion of the group of coupled soil nodes was limited to that of the rigid body. The advantage of this method is that it avoids (a) the extremely thin columns of elements required for modelling internal skirts explicitly ($t \approx 0.1\%B$ in reality), and (b) the contact iterations associated with the soil-skirt interface. Therefore, the current models for skirted foundations are more time-efficient and stable than if internal skirts are represented explicitly.

2.2 Material properties and interface conditions

The undrained shear strength of the soil was modelled as either uniform with depth or increasing linearly with depth according to $s_u = s_{um} + kz$, where s_{um} is the shear strength at the

mudline and k is the shear strength gradient with depth, z (Figure 1). The soil heterogeneity is described by the dimensionless index $\kappa = kB/s_{um}$ where 0 represents a uniform strength with depth and ∞ a linearly increasing strength with depth with essentially zero mudline strength intercept, i.e. normally consolidated. A range of $0 \leq \kappa \leq \infty$ was considered to cover the whole range of linearly increasing profiles with intermediate values of κ = 2, 5, 8, 10, 20, 30 and 100. It is also convenient to consider the local shear strength heterogeneity in the vicinity of the skirt tips, which can be defined by $k_d = kd/s_{u0}$, where $s_{u0} = s_{um} + kd$. The value of k_d is constrained to lie between 0 (homogeneous) and 1 (zero strength intercept at mudline).

The soil was modelled as linear elastic, perfectly plastic obeying a Tresca failure criterion to make straightforward comparison with the previous published data to validate the present finite element model. The shear strength would be adjusted appropriately if a von Mises criterion was used. For a square foundation, Tresca analysis predicts 3% higher vertical capacity compared with von Mises (based on plane strain, or simple shear, strength) and the disparity diminishes as the foundation length increases until the solution converges for plane strain conditions [10]. The elastic properties were defined by undrained Young's modulus $E = 1000s_u$ and Poisson's ratio of $\nu = 0.49$ (to avoid numerical difficulties associated with the constant-volume response of soil under truly undrained conditions). This gives a relatively high rigidity index G/s_u of 336, where G is the shear modulus of the soil, so that failure occurs at relatively small displacements to avoid problems of mesh distortion.

The interface between the underside of the rigid solid plug foundation and the subsoil was taken to be rough in shear with no detachment between the mudmat and soil permitted (i.e. fully bonded) to represent the 'rough' soil-soil interface at skirt tip level of a skirted foundation. The inside faces of the peripheral skirts and the underside of the foundation base plate of the skirted foundations were also prescribed a fully bonded interface with the soil. For the solid plug and skirted foundations, the contact between the external face of the peripheral skirts and the adjacent soil was modelled as frictionless with separation permitted under tensile normal stress at the interface, providing a conservative prediction of capacity.

2.3 Load path

The response of the mudmat foundations subjected to V-H^2-M^2-T loading is presented in the form of failure envelopes. Failure envelopes under combined loading conditions are generally evaluated through swipe tests or fixed ratio displacement probe tests, implemented using the general static procedures in ABAQUS. Sideswipe tests, which have been used in previous

experimental and numerical work, take advantage of allowing large sections of failure envelope to be investigated in a single analysis, see e.g. Refs. [9, 16]. However, fixed ratio displacement controlled probe tests were carried out in this study because the load path in a sideswipe test can undercut the true failure envelope, particularly for embedded foundations [7]. For general V-H^2-M^2-T loading, a constant vertical load, expressed as a proportion of the ultimate vertical capacity of a solid foundation, was imposed and the horizontal load, moment or torsion components were applied as a series of displacement probes to detect each failure envelope. Failure envelopes were derived for foundation embedment ratios d/B = 0.05, 0.1 and 0.2, for various degrees of shear strength heterogeneity over the range $0 \leq \kappa \leq \infty$, in planes of V/V_{ult} = 0, 0.25, 0.5 and 0.9, where V_{ult} is taken as the ultimate vertical bearing capacity of the solid rigid foundation with equal embedment ratio to the corresponding skirted foundations.

3. RESULTS

3.1 Validation of FE Model

The three dimensional finite element models were validated by comparing the predicted vertical bearing capacity with analytical plasticity solutions for rectangular and square mudmat foundations on homogenous soil ($\kappa = 0$) as shown in Table 1. The bearing capacity factors for strip foundations obtained from FE analysis over-predict the numerical upper bound solutions [14] by approximately 2%. The FE results of vertical bearing capacity for the three-dimensional foundation geometry are bracketed by the lower and upper bound values, due to lower overestimation of the true collapse loads, as a result of smoothing of the Tresca yield surface in Abaqus [15].

The modelling of the internal skirts using kinematic coupling constraints instead of being implemented explicitly was also verified. An example is presented in Figure 4 showing the failure envelope for a skirted foundation on heterogeneous soil with kB/s_{um} = 100 under combined H_x-M_y loading along with several selected loading paths, which are the reactive forces obtained from different displacement controlled probe tests represented by a non-dimensional parameter $p = u_x/(B\theta_y)$. In the analyses, the foundation had one internal skirt in each direction, simulated in two separated models in the form of implicit and explicit skirts. The ‘implicit’ and ‘explicit’ skirts refer to skirts modelled respectively either by kinematically constrained soil nodes or by discretisation using continuum solid elements. The identical loading paths and failure points for skirted foundations with implicit and explicit skirts are

evident for any given value of p. Therefore, the kinematic coupling constraint method is effective without compromising accuracy.

3.2 In-plane V-M-H loading

The optimal internal skirt spacing for mudmat foundations subjected to in-plane V-M-H loading was explored first. Figure 5 and Figure 6 shows the combined H-M loading capacity for rectangular foundations, B/L = 0.5, with an embedment ratio d/B = 0.1, for kB/s_{um} = 0, 2, 30, 100 and ∞, in a plane of V/V_{ult} = 0.5 for a solid foundation and skirted foundations with different numbers of internal skirts. Skirt configuration B*n*L*n* denotes n internal skirts along the breadth (B) and length (L) of the foundation. As shown in Figure 5 and Figure 6, the innermost failure envelope corresponds to a foundation with peripheral skirts only, which is referred to as having zero internal skirts or B0L0. The outermost failure envelope corresponds to the solid foundation defining the maximum load-carrying capacity. The addition of internal skirts leads to expansion of the HM failure envelope, indicating the increase of load-carrying capacity. The optimal number of internal skirts was determined as when the failure envelope of the skirted foundation coincided with that of a solid foundation or when the increase of capacity of a skirted foundation with n and n+1 internal skirts was negligible. For example, the skirt configurations B2L2 and B3L3 were considered to be sufficient to mobilise the maximum H_x-M_y load-carrying capacity for soil strength profile linearly increase with depth with kB/s_{um} = 2 and 100, respectively, for vertical load mobilisation V/V_{ult} = 0.5.

The failure envelopes allow selection of example loading paths to show the transformation of soil failure mechanisms for different internal skirt spacings. Two such paths are shown in Figure 5b and Figure 5d. Figure 7 and Figure 8 illustrate selected failure mechanisms at the midline cross-section of the foundation for in-plane V-M_y-H_x loading for rectangular foundations with embedment ratio d/B = 0.1 considering soil heterogeneity $\kappa = kB/s_{um}$ = 2 and 100. The comparison of soil flow vectors for solid foundation and skirted foundations shows the transition in failure mechanisms with additional internal skirts, up to the point where the soil plug remains intact. The load combinations corresponding to the failure mechanisms in Figure 7 and Figure 8 are indicated in the failure envelopes by the constant M_y/BH_x load path in Figure 5b and Figure 5d, respectively.

3.3 V-M^2-H^2-T loading

External loads applied to subsea structures often result in loading in six degrees-of-freedom being transferred to the mudmat. It is therefore important to identify the controlling load

case(s) for determining the optimal spacing of internal skirts. The critical load case was identified for the range of conditions considered in this study.

The procedure to verify the governing case is demonstrated below for an example of a rectangular foundation with embedment ratio d/B = 0.1. Figure 9 shows the biaxial horizontal loading capacity for solid and skirted foundations in the absence of vertical load. It can be seen that a single internal skirt along the breadth and length of the skirted foundation is required to mobilise the maximum horizontal capacity, irrespective of the direction of horizontal loading. Figure 10 shows the failure envelopes for combined H_x-T and H_y-T loading and indicates that the optimal combined horizontal and torsional capacity is also achieved with a single internal skirt along the breadth and length of the foundation. It is to be expected that the required number of internal skirts is the same under biaxial horizontal and torsional-horizontal loading since the failure mechanisms are governed by soil shearing at skirt tip level and passive and active soil failure against the skirts in both modes [13]. For the combined H-T loading, which is generated by an eccentrically applied horizontal load, the additional resistance provided by the skirts can never be larger than that to mobilise the maximum horizontal capacity. Therefore, if the skirt configuration of B1L1 is sufficient for maximum horizontal capacity, it must suffice to mobilise the maximum combined H-T capacity. By contrast, two or three skirts are required along the breadth and length of the foundation to achieve optimal moment capacity, as indicated by the failure envelopes for biaxial moment capacity shown in Figure 11.

Table 2 summarises the number of internal skirts required for optimal capacity in all planes of loading in the absence of vertical load. It is apparent that the greatest number of internal skirts is generally that required for mobilising maximum combined $H_{x(y)}$-$M_{y(x)}$ loading capacity. The number of internal skirts required for maximum load-carrying capacity has been shown to increase with increasing vertical load mobilisation for plane strain conditions [11] and is verified in this study, as illustrated later in Figure 15. Therefore, it is concluded that in-plane V-M-H loading is the critical case for determining optimal internal skirt spacing and it may be asserted that the critical number of internal skirts for mudmats subjected to in-plane V-M-H loading can be used for selection of internal skirt spacing for mudmats under V-H^2-M^2-T loading.

3.4 Effects of foundation shape and roughness on optimal number of internal skirts

The optimal number of internal skirts for strip foundations was analysed to investigate the effect of foundation shape. Figure 12 shows failure envelopes for foundations with different

breadth to length aspect ratios, B/L, but the same equivalent embedment ratio under in-plane V-M-H loading, on soil with $kB/s_{um} = 100$. It can be seen that the number of internal skirts for maximum capacity was generally the same for a given equivalent embedment ratio (i.e. d/B for loading in a plane parallel to the shorter side, and d/L for the plane parallel to the longer side), irrespective of the breadth to length aspect ratio. Figure 13 demonstrates similarity of the soil failure mechanisms for a rectangular foundation and strip foundation with equivalent embedment ratio and the same number of internal skirts under a selected M-H load path of $M/BH = 1.5$, for given vertical load mobilisation, $V/V_{ult} = 0.5$, reflecting the observations from the failure envelopes. The similarity arises as the horizontal and moment failure mechanisms are essentially in-plane and hence independent of the length to breadth aspect ratio of the foundation. As load combinations involve significant vertical load mobilisation, soil failure mechanism may extend in the out-of-plane directions for three-dimensional foundation geometry and the comparison with plane strain conditions would become marked. Therefore, plane strain analysis can be used to determine the optimal number of internal skirts using the relevant embedment ratio, d/B or d/L, according to the plane of loading being considered for rectangular mudmats.

The effect of interface roughness of the internal skirts on the optimal number of skirts for maximum capacity was explored by comparing results for this study with results for strip foundations with all smooth interfaces, including the skirt-soil interface and at the underside of the base plate [11]. A comparison is shown in Figure 14 and in general one additional skirt is required for foundations with a completely smooth foundation-soil interface to mobilise the maximum available capacity. The additional skirt is required due to the reduced resistance at the underside of the foundation plate in the skirted compartment and the effect becomes less pronounced with increasing foundation embedment ratio as the failure mechanism is pushed towards skirt tip level.

3.5 Design guidance

Figure 15 provides a practical guide for determining the optimal number of internal skirts for subsea mudmats as a function of equivalent foundation embedment ratio, soil strength heterogeneity index and vertical load mobilisation. The equivalent embedment ratio is taken as d/B for defining the number of internal skirts across the foundation breadth and d/L for defining the number of internal skirts across the foundation length of a rectangular mat. The critical number of internal skirts is seen to increase with decreasing foundation embedment ratio, increasing soil heterogeneity index and increasing level of vertical load mobilisation.

The required number of internal skirts described by constant skirt spacing to skirt depth ratio, s/d, is also shown. A value of s/d = 5, commonly taken as a rule of thumb for skirt spacing, over estimates the critical number of internal skirts for cases of low vertical load mobilisation, low soil heterogeneity index and low embedment ratio but becomes unconservative with increasing vertical load mobilisation, soil heterogeneity index and foundation embedment ratio. An s/d ratio of unity, as recommended by Thompson et al. (2011) [17], is shown to over predict the required number of skirts for all conditions.

Equivalently, the optimal internal skirt spacing ratio, s/B = 1/(n+1) (or equivalent for s/L), may be plotted as a function of the local soil heterogeneity index, $\kappa_d = kd/s_{u0}$, focusing on the local shear strength gradient relative to the local strength within the skirt compartment. Figure 16 shows that the optimal skirt spacing varies from approximately 0.33 (though potentially as high as 0.5 at low vertical load) at low κ_d down to around 0.2 at high κ_d but with some dependence on vertical load level and embedment ratio.

The optimal internal skirts spacing indicated in Figure 15 and Figure 16 was determined, as defined at the outset, as when the failure envelope of the skirted foundation coincided with that of a solid foundation or when the increase in capacity of a skirted foundation with n and n+1 internal skirts was negligible. It is acknowledged that engineering judgment may be used to determine a less stringent criterion, but this would be the responsibility of the designer on a case by case basis.

The guidance provided here is valid for the conditions considered, in particular for soil profiles with linearly increasing shear strength with depth, as commonly encountered in deepwater seabeds. Seabeds in some regions may exhibit a crust at mudline level overlying a deposit with linearly increasing strength profile. Individual consideration should be given to soil conditions outside those considered in this study.

4. CONCLUSIONS

This paper presents results from finite element analyses of the undrained capacity of subsea skirted mudmats under V-H^2-M^2-T loading. The optimal number of internal skirts for maximum capacity has been presented as simple to use design charts as a function of skirt embedment ratio, soil strength heterogeneity index and vertical load mobilisation. The effects of three dimensional foundation geometry and skirt interface roughness were also quantified. In summary, the results have shown that:

- Internal skirts of mudmat foundations can be effectively modelled by kinematic coupling constraint techniques.
- In-plane V-M-H loading is the governing load combination in terms of determining the required skirt spacing for skirted mudmat foundations under general V-H^2-M^2-T loading.
- More internal skirts are required to mobilise maximum capacity of skirted mudmat foundations if the foundation underside and internal skirt-soil interface is smooth as opposed to rough particularly at low embedment ratios.
- Plane strain analysis can be used to predict the critical number of internal skirts along the breadth and length of a rectangular foundation using equivalent foundation embedment ratios of d/B and d/L.
- Simple to use charts can provide design guidance on the critical number of skirts, or equivalent skirt spacing, for optimal foundation capacity under V-H^2-M^2-T loading as a function of normalised skirt embedment ratio, soil strength heterogeneity index and level of vertical load mobilisation.

Although the primary focus of the paper has been to identify the critical number of skirts to guarantee maximum capacity of the foundation, results may also be implemented in simple models that quantify the reduction in capacity for foundations containing fewer internal skirts than critical.

5. ACKNOWLEDGEMENTS

This work forms part of the activities of the Centre for Offshore Foundation Systems (COFS), currently supported as a node of the Australian Research Council Centre of Excellence for Geotechnical Science and Engineering and as a Centre of Excellence by the Lloyd's Register Foundation. Lloyd's Register Foundation helps to protect life and property by supporting engineering-related education, public engagement and the application of research. Part of the research presented here derives from a collaboration between COFS, Subsea 7 and BP. The authors also acknowledge the valuable comments and suggestions from the reviewers.

REFERENCES

[1] Bransby MF, Randolph MF. Combined loading of skirted foundations. Geotechnique. 1998; 48(5):637-55.
[2] Bransby MF, Randolph MF. The effect of embedment depth on the undrained response of skirted foundations to combined loading. Soil Found. 1999; 39(4):19-33.

[3] Bransby MF, Yun GJ. The undrained capacity of skirted strip foundations under combined loading. Géotechnique. 2009; 59(2):115-25.
[4] USA.Abaqus analysis users' manual.Simulia Corp, Providence, RI:2010.
[5] Feng X, Gourvenec S. Optimal shear key interval for offshore shallow foundations. In: Proc of The 32nd Int Conf on Ocean, Offshore and Arctic Engineering (OMAE 2013). Nantes, France, 2013. p. 308-17.
[6] Feng X, Randolph MF, Gourvenec S, Wallerand R. Design approach for rectangular mudmats under fully three-dimensional loading. Geotechnique. 2014; 64(1):51-63.
[7] Gourvenec S. Effect of embedment on the undrained capacity of shallow foundations under general loading. Géotechnique. 2008; 58(3):177-85.
[8] Gourvenec S, Barnett S. Undrained failure envelope for skirted foundations under general loading. Géotechnique. 2011; 61(3):263-70.
[9] Gourvenec S, Randolph M. Effect of strength non-homogeneity on the shape of failure envelopes for combined loading of strip and circular foundations on clay. Geotechnique. 2003; 53(6):575-86.
[10] Gourvenec S, Randolph M, Kingsnorth O. Undrained bearing capacity of square and rectangular footings. Int J Geomech. 2006; 6(3):147-57.
[11] Mana D, Gourvenec S, Martin C. Critical Skirt Spacing for Shallow Foundations under General Loading. J Geotech Geoenviron Eng ASCE. 2013; 139(9):1554-66.
[12] Mana DSK, Gourvenec S, Randolph MF. A numerical study of the vertical bearing capacity of skirted foundations. In: Proc of The 2nd Int Symp on Front in Offshore Geotech (ISFOG 2010). Perth, Australia, 2010. p. 433-8.
[13] Murff JD, Aubeny CP, Yang M. The effect of torsion on the sliding resistance of rectangular foundations. *2nd Int Symp on Front in Offshore Geotech (ISFOG 2010)*. Perth, Australia2010. p. 439-43.
[14] Salgado R, Lyamin AV, Sloan SW, Yu HS. Two- and three-dimensional bearing capacity of foundations in clay. Géotechnique. 2004; 54(5):297-306.
[15] Taiebat H, Carter J. Flow rule effects in the Tresca model. Comput Geotech. 2008; 35(3):500-3.
[16] Tan FS. Centrifuge and theoretical modelling of conical footings on sand. PhD Thesis, University of Cambridge, UK, 1990.
[17] Thompson D, Rocker J, Jung B, Briaud J-L, Lin S. Handbook for Marine Geotechnical Engineering: Naval Facilities Engineering Service Centre; 2011.
[18] Yun G, Bransby MF. The horizontal-moment capacity of embedded foundations in undrained soil. Can Geotech J. 2007; 44(4):409-24.

TABLE CAPTIONS

Table 1 Comparison of vertical bearing capacity calculated by FE and plasticity analysis for uniform soil strength, $kB/s_{um} = 0$

Table 2 Optimal number of internal skirts along breadth and length of a rectangular mudmat under various loading conditions, $kB/s_{um} = 100$, $V/V_{ult} = 0$

FIGURE CAPTIONS

Figure 1 Nomenclature for foundation geometry, general loading and soil strength profile

Figure 2 FE mesh for rectangular mudmats d/B = 0.1, B/L= 0.5 - half mesh with plane of symmetry through foundation centreline

Figure 3 Schematic of skirted foundations and implicit modelling of internal skirts

Figure 4 Comparison of loading paths and failure envelope for a skirted foundation using explicit and implicit internal skirts: $kB/s_{um} = 100$ and $d/B = 0.1$

Figure 5 Failure envelopes for mudmat foundation under in-plane V-H_x-M_y loading, d/B = 0.1

Figure 6 Failure envelopes for mudmat foundation under in-plane V-H_y-M_x loading, d/B = 0.1

Figure 7 Kinematic failure mechanisms for $kB/s_{um} = 2$ and $d/B = 0.1$; loading $V/V_{ult} = 0.5$; $M_y/BH_x = 1.5$

Figure 8 Kinematic failure mechanisms for $kB/s_{um} = 100$ and $d/B = 0.1$; loading $V/V_{ult} = 0.5$; $M_y/BH_x = 1.5$

Figure 9 Failure envelopes for mudmat foundations under biaxial horizontal loading, kB/s_{um} =100 and d/B = 0.1

Figure 10 Failure envelopes for mudmat foundations under combined H-T loading, kB/s_{um} = 100 and d/B =0.1

Figure 11 Failure envelopes for mudmat foundations under biaxial moment loading, kB/s_{um} = 100 and d/B = 0.1

Figure 12 Failure envelopes for different foundation shapes with equivalent embedment ratio, $kB/s_{um} = 100$

Figure 13 Comparison of failure mechanisms for rectangular and strip foundation, kB/s_{um} = 100

Figure 14 Effect of roughness of internal skirts and underside of foundation baseplate on optimal number of internal skirts

Figure 15 Optimal number of internal skirts for subsea mudmats under V-H^2-M^2-T loading

Figure 16 Optimal skirt spacing as a function of local soil strength heterogeneity, kd/s_{u0}

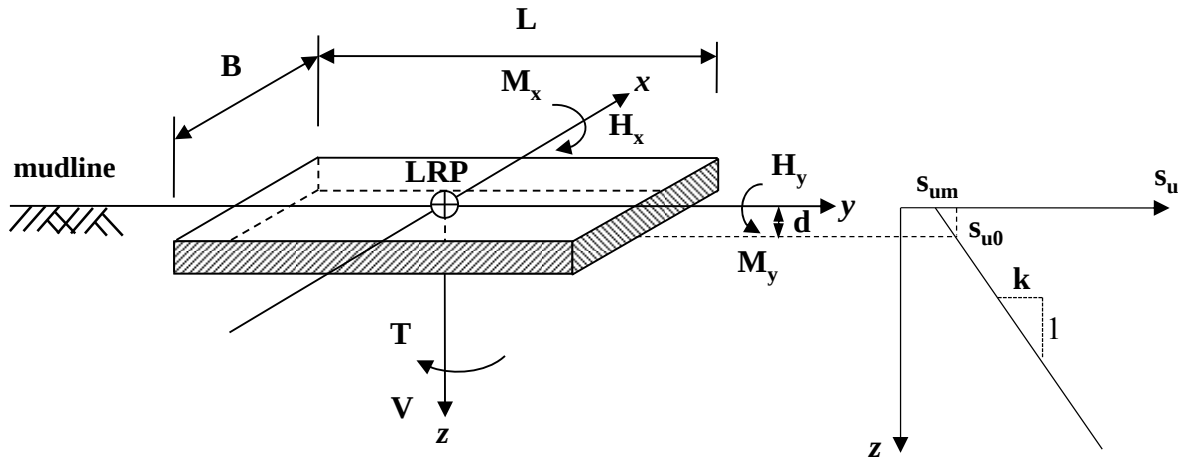

Figure 1 Nomenclature for foundation geometry, general loading and soil strength profile

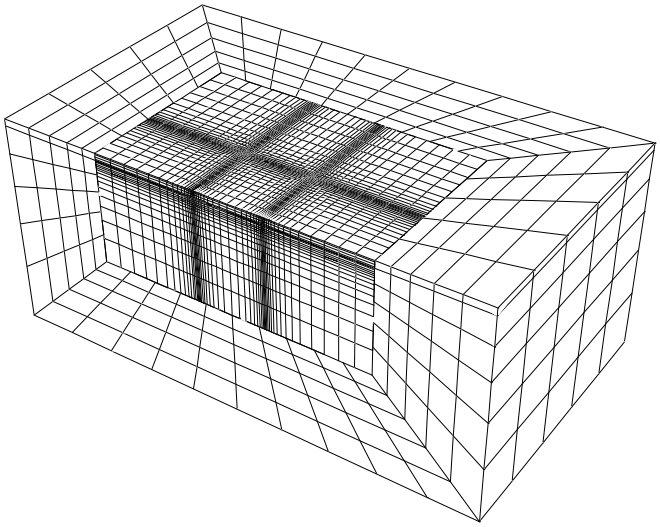

(a) FE mesh

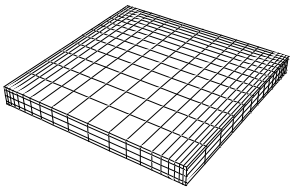

(b) Solid foundation

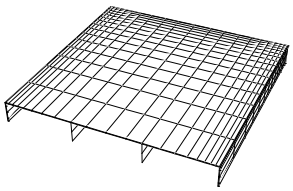

(c) Skirted foundation

Figure 2 FE mesh for rectangular mudmats d/B = 0.1, B/L= 0.5 - half mesh with plane of symmetry through foundation centreline

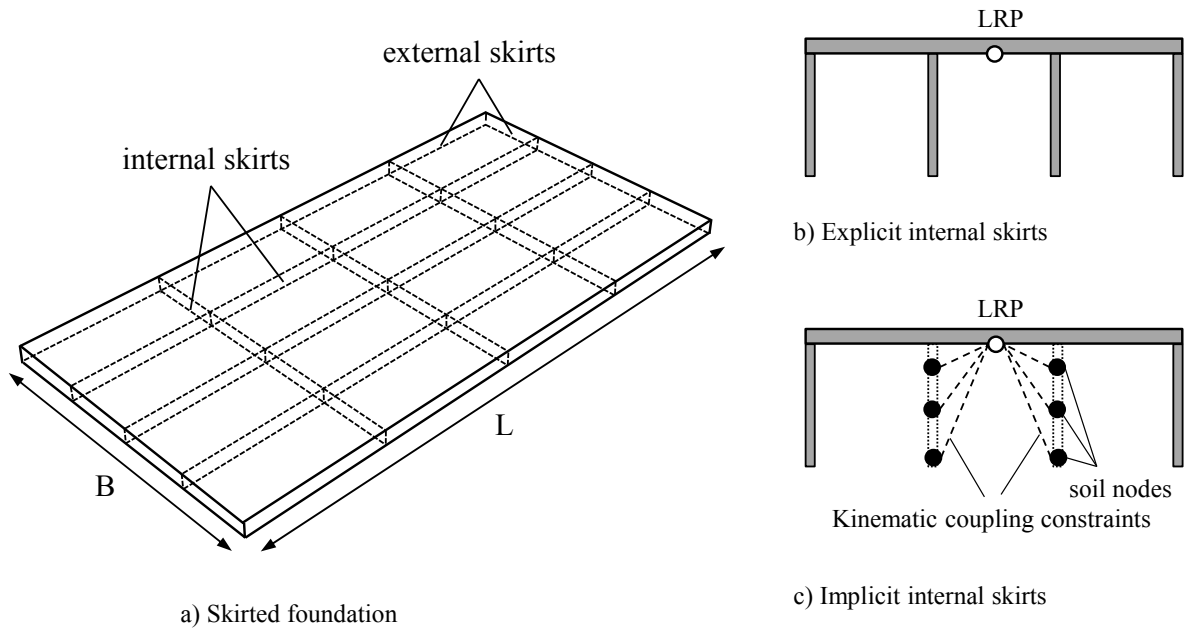

Figure 3 Schematic of skirted foundations and implicit modelling of internal skirts

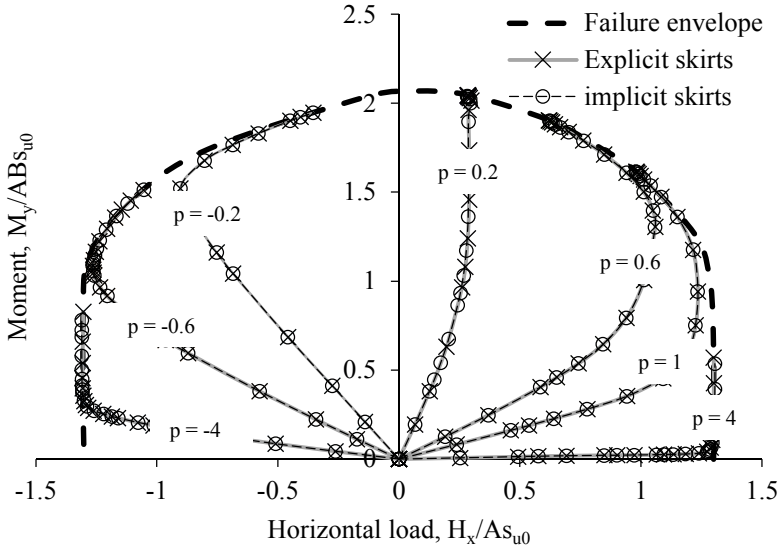

Figure 4 Comparison of loading paths and failure envelope for a skirted foundation using explicit and implicit internal skirts: $kB/s_{um} = 100$ and $d/B = 0.1$

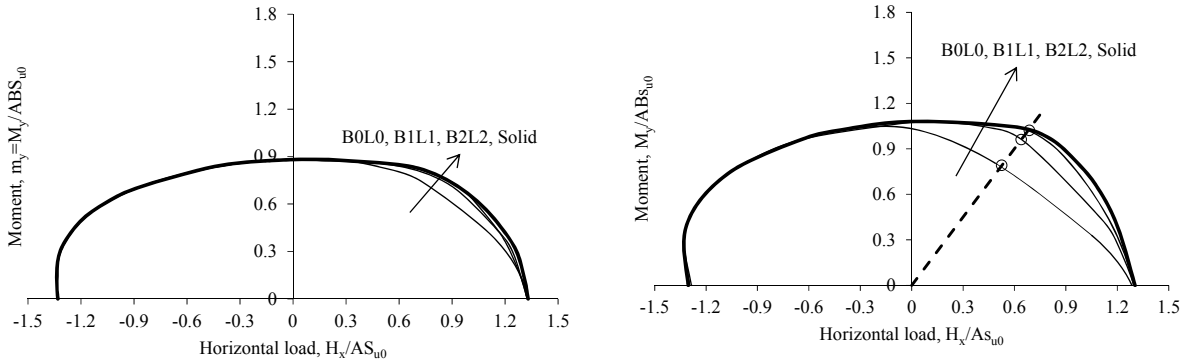

(a) $\kappa = 0$ (b) $\kappa = 2$

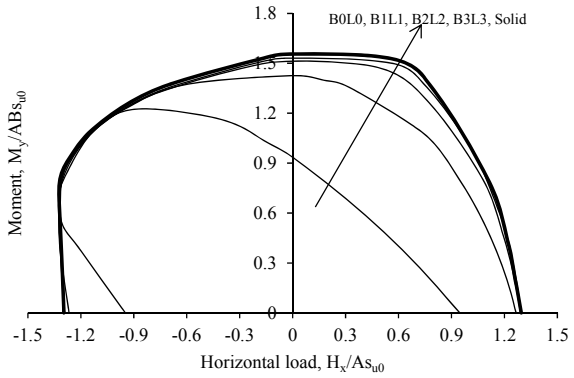

(c) κ = 30

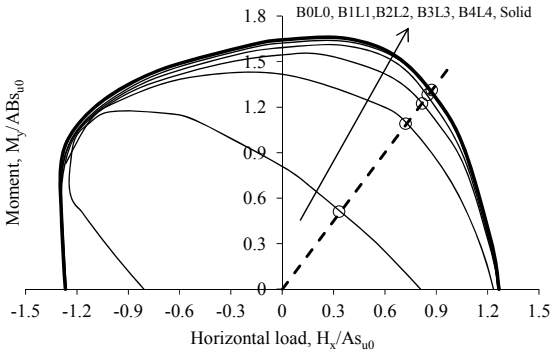

(d) κ = 100

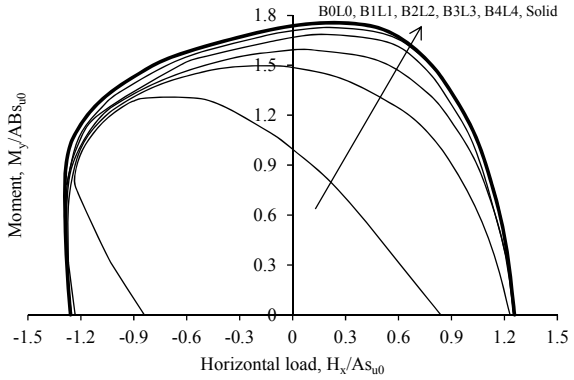

(e) κ = ∞

Figure 5 Failure envelopes for mudmat foundation under in-plane V-H_x-M_y loading, d/B = 0.1

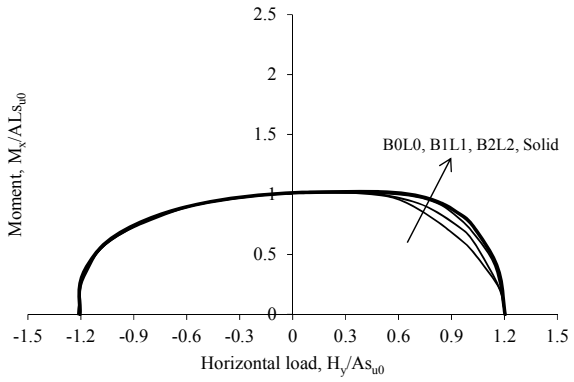

(a) κ = 0

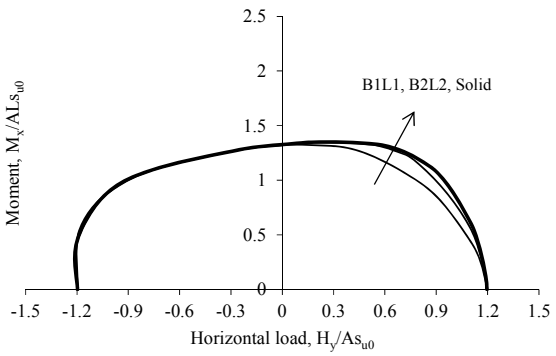

(b) κ = 2

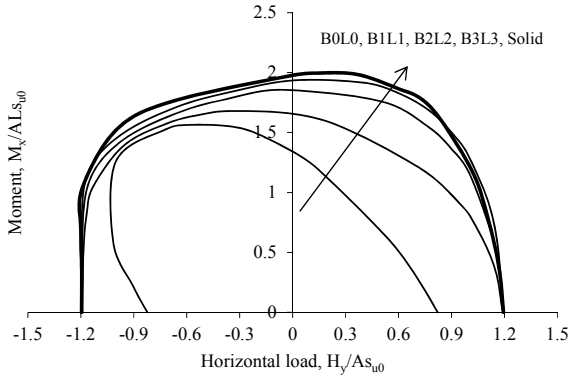

(c) κ = 30

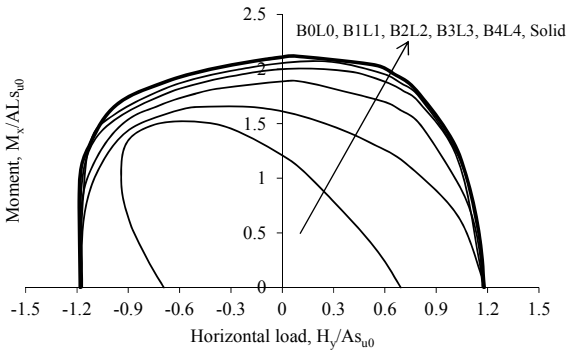

(d) κ = 100

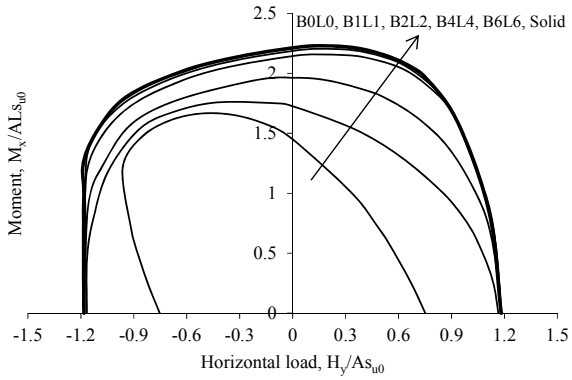

(e) $\kappa = \infty$

Figure 6 Failure envelopes for mudmat foundation under in-plane V-H_y-M_x loading, d/B = 0.1

(a) Skirted B0L0 (b) Skirted B1L1

(c) Skirted B2L2 (d) Solid plug

Figure 7 Kinematic failure mechanisms for $kB/s_{um} = 2$ and d/B = 0.1; loading $V/V_{ult} = 0.5$; $M_y/BH_x = 1.5$

(a) Skirted B0L0 (b) Skirted B1L1

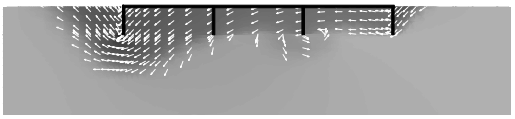

(c) Skirted B2L2

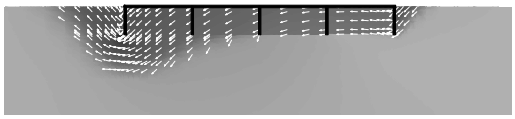

(d) Skirted B3L3

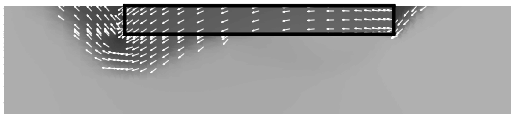

(e) Solid plug

Figure 8 Kinematic failure mechanisms for kB/s_{um} = 100 and d/B = 0.1; loading V/V_{ult} = 0.5; M_y/BH_x = 1.5

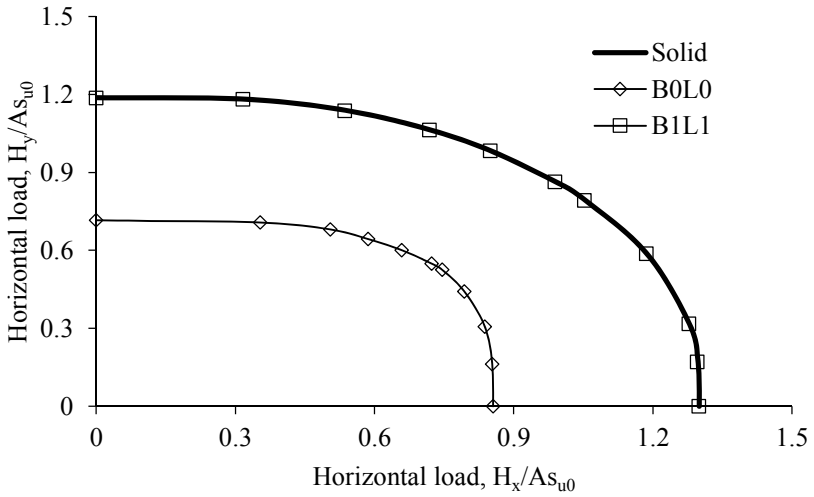

Figure 9 Failure envelopes for mudmat foundations under biaxial horizontal loading, kB/s_{um} =100 and d/B = 0.1

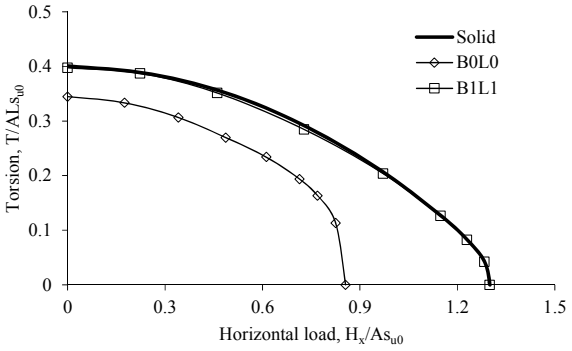

(a) Combined H_x-T loading

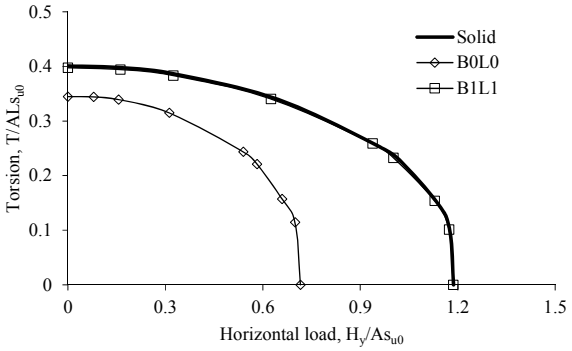

(b) Combined H_y-T loading

Figure 10 Failure envelopes for mudmat foundations under combined H-T loading, kB/s_{um} = 100 and d/B =0.1

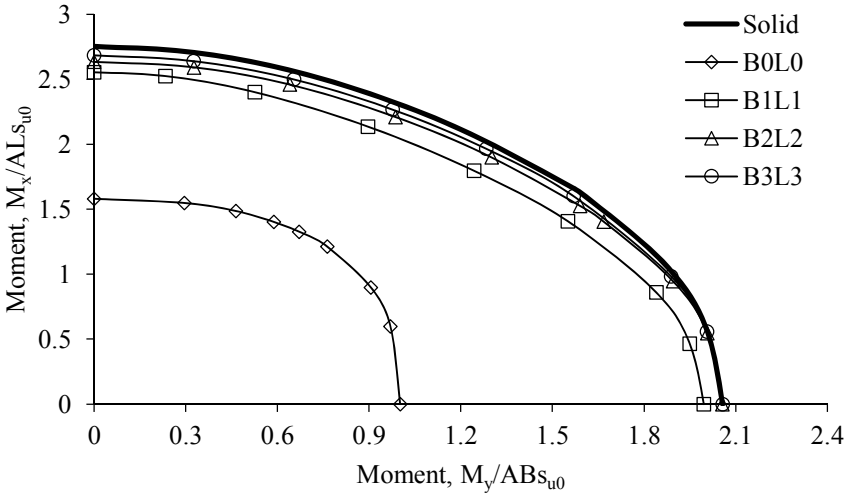

Figure 11 Failure envelopes for mudmat foundations under biaxial moment loading, kB/s_{um} = 100 and d/B = 0.1

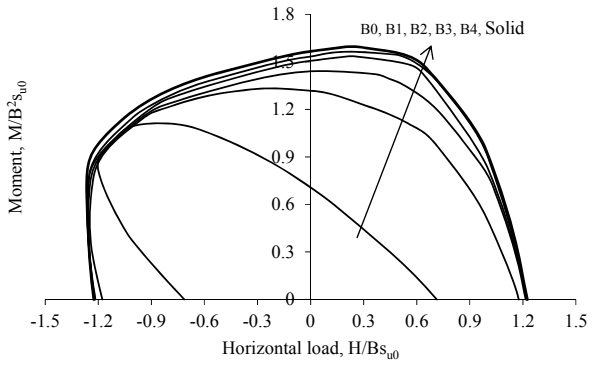

(a) B/L = 0; d/B = 0.1

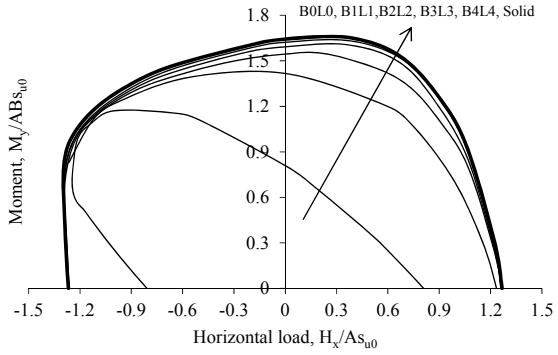

(b) B/L = 0.5; d/B = 0.1

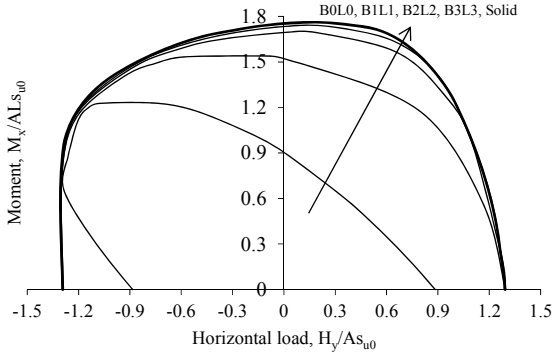

(c) B/L = 0.5; d/L = 0.1 (d/B = 0.2)

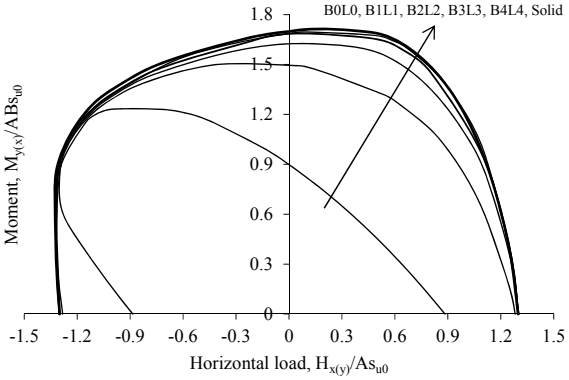

(d) B/L = 1; d/B = 0.1

Figure 12 Failure envelopes for different foundation shapes with equivalent embedment ratio, kB/s_{um} = 100

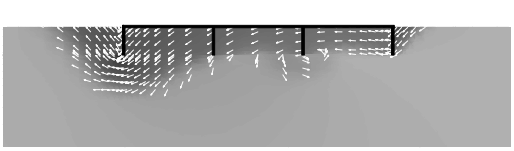

(a) Rectangular: midpoint section

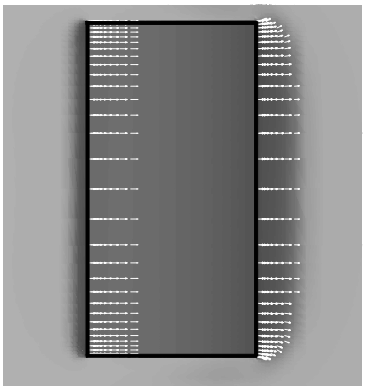

b) Rectangular: plan view

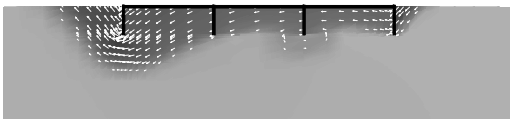

c) Strip

Figure 13 Comparison of failure mechanisms for rectangular and strip foundation, kB/s_{um} = 100

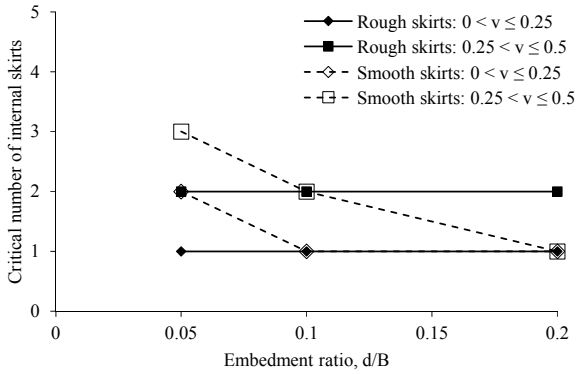

(a) $kB/s_{um} = 0$

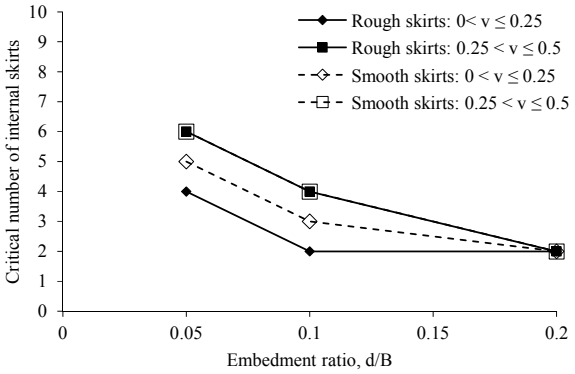

(b) kB/sum = ∞

Figure 14 Effect of roughness of internal skirts and underside of foundation baseplate on optimal number of internal skirts

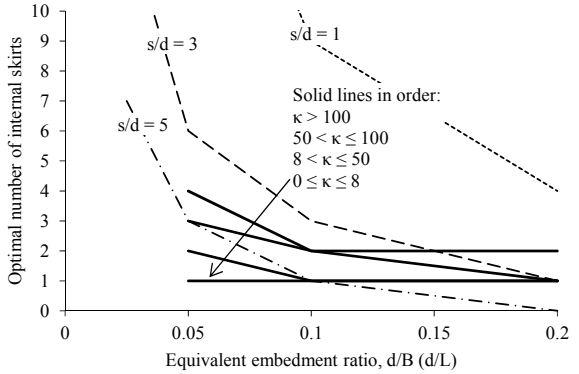

(a) $V/V_{ult} \leq 0.25$

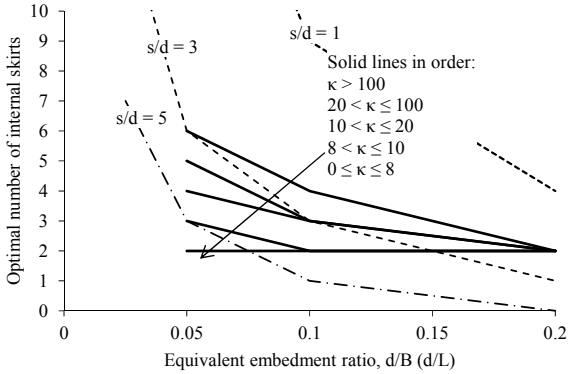

(b) $0.25 < V/V_{ult} \leq 0.5$

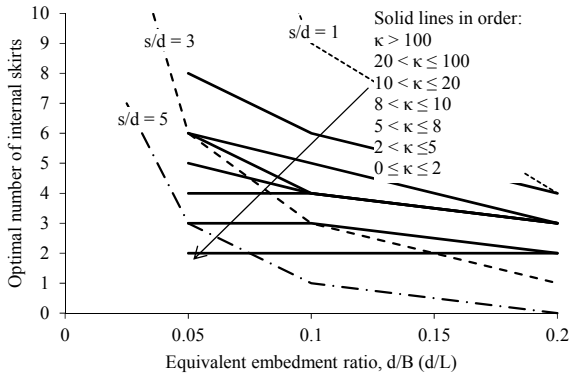

(c) $0.5 < V/V_{ult} \leq 0.9$

Figure 15 Optimal number of internal skirts for subsea mudmats under V-H^2-M^2-T loading

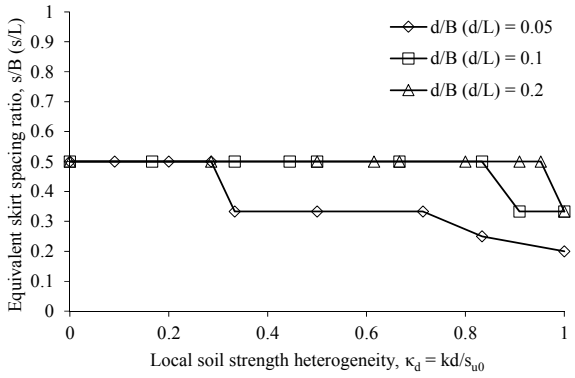

(a) $V/V_{ult} \leq 0.25$

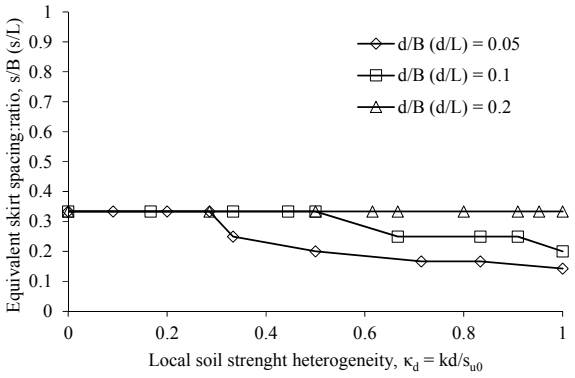

(b) $0.25 < V/V_{ult} \leq 0.5$

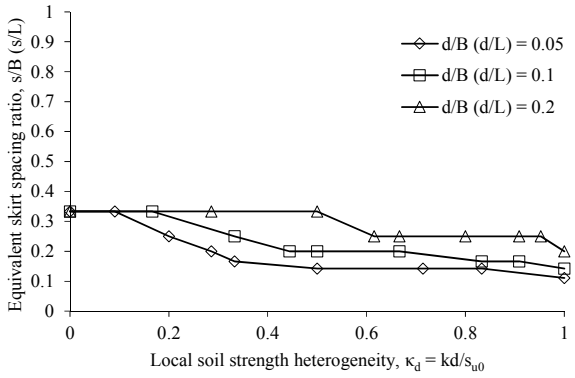

(c) $0.5 < V/V_{ult} \leq 0.9$

Figure 16 Optimal skirt spacing as a function of local soil strength heterogeneity, kd/s_{u0}